Dalton Transactions

ROYAL SOCIETY OF CHEMISTRY

COMMUNICATION

View Article Online
View Journal | View Issue

Check for updates

Cite this: *Dalton Trans.*, 2025, **54**, 12135

Received 3rd June 2025,
Accepted 2nd July 2025

DOI: 10.1039/d5dt01302j

rsc.li/dalton

Synthesis and characterization of *closo*-decahydrido-decaborate-phosphine mediated by palladium(0) complexes†

Zainab Haidar Ahmad,[a,b] Marie Cordier,[a] Daoud Naoufal*[b] and Christophe Darcel *[a]

We report an efficient and selective preparation of an apical mono-functionalized *closo*-decahydrido-decaborate anion $[B_{10}H_{10}]^{2-}$ with aromatic or aliphatic tertiary phosphines. Starting from $[N(n\text{-}C_4H_9)_4]_2[1\text{-}B_{10}H_9I]$ and 0.25–0.5 equiv. of Pd(0)-PR_3, the corresponding $[N(n\text{-}C_4H_9)_4][1\text{-}B_{10}H_9PR_3]$ compounds were obtained in high isolated yields under mild conditions. Additionally, a plausible mechanism was proposed based on experimental evidence.

Introduction

In the area of boron cluster chemistry,[1] the decaborate anion, $[B_{10}H_{10}]^{2-}$, exhibits a 3D aromaticity, leading to unusual oxidative, hydrolytic and thermal stabilities.[1] It is also described as exhibiting a non-uniform electronic distribution within the cage and the charges of atoms in this cluster differ for different vertices (apical *vs.* equatorial).[2–4] These properties make such clusters susceptible to both nucleophilic and electrophilic substitutions.[4] More precisely, the activation of the *exo*-B–H bond in the polyhedral *closo*-decahydrido-decaborate anion $[B_{10}H_{10}]^{2-}$ has been a subject of intensive investigation in the last few decades.[5–9] Indeed, its derivatives have applications in medicine—notably in boron neutron capture therapy[10,11]—materials sciences,[12] ion extraction systems,[13] and aerogel nanomaterial preparation,[14] as solid and liquid electrolytes[15] and in tunable intermolecular charge transfer.[16] However, selective heterofunctionalization of this cluster, notably with organophosphorus motifs, still remains challenging in terms of regioselectivity and efficiency. Earlier attempts to prepare mono-substituted phosphine derivatives have been largely restricted to $[B_{12}H_{12}]^{2-}$[17–19] and carbaboranes.[20,21] In the case of the $[B_{10}H_{10}]^{2-}$ anion, the scarce reports dealing with phosphine functionalization often exhibit poor regioselectivity and formation of a mixture of mono-, di- and/or polysubstituted products.[22] In 1994, Todd and co-workers reported the synthesis of the 1,10-, 1,6- and 1,7(8) isomers of $(PMe_2Ph)_2B_{10}H_8$ in low yields using 2.5 equiv. of $(PMe_2Ph)_2PdCl_2$.[23] In 1999, Naoufal *et al.* reported that the combination of $(PPh_3)_2PdCl_2$ and CuI catalysts promoted the substitution of the diazo group in $[1\text{-}N_2B_{10}H_9]^-$ by diphenylphosphine, leading to $[1\text{-}(Ph_2PH)B_{10}H_9]^-$ species in a mixture with $[1\text{-}Ph_2P(OH)B_{10}H_9]^-$.[17] It is worth underlining that all these previous preparations required long and difficult synthetic procedures even if several products were obtained despite their tedious purification.

Based on a pioneering result of one of our research groups on the palladium promoted preparation of one example of *closo*-$[1\text{-}B_{12}H_{11}PPh_3][Nn\text{-}Bu_4]_2$ from *closo*-$[1\text{-}IB_{12}H_{11}][Nn\text{-}Bu_4]_2$,[24] we report herein a general and easy palladium-promoted synthesis of $[N(n\text{-}C_4H_9)_4][1\text{-}B_{10}H_9PR_3]$ from $[N(n\text{-}C_4H_9)_4]_2[1\text{-}B_{10}H_9I]$ using tertiary phosphines.

Results and discussion

Synthesis of *closo*-decahydrido-decaborate-phosphine clusters

The preparation of mono-anionic tertiary phosphine derivatives of the *closo*-decahydrido-decaborate cluster was first evaluated starting from a commercially available palladium precursor such as $Pd(PPh_3)_4$. Indeed, starting from 1 equiv. of iodinated boron cluster $[N(n\text{-}C_4H_9)_4]_2[1\text{-}B_{10}H_9I]$ **1**,[22] in the presence of 10 mol% of $Pd(PPh_3)_4$ and 3 equiv. of Na_2CO_3 in dried and degassed THF at 50 °C for 2 h, the corresponding $[N(n\text{-}C_4H_9)_4][1\text{-}B_{10}H_9(PPh_3)]$ **2a** was obtained in 33% isolated yield (conv. = 40%). When increasing the amount of Pd(0) to 25 mol% (*i.e.*, 1 equimolar amount of triphenylphosphine), full conversion was achieved and **2a** was isolated in 80% yield. Noticeably, the reaction can be conducted with similar

[a]*Univ. Rennes, CNRS, ISCR UMR 6226, F-35000 Rennes, France. E-mail: christophe.darcel@univ-rennes.fr*
[b]*Inorganic and Organometallic Coordination Chemistry Laboratory, Lebanese University, Lebanon. E-mail: dnaoufal@ul.edu.lb*

† Electronic supplementary information (ESI) available. CCDC 2456501–2456506. For ESI and crystallographic data in CIF or other electronic format see DOI: https://doi.org/10.1039/d5dt01302j

efficiency in different solvents, including CH_2Cl_2, 1,4-dioxane and acetonitrile. It should be noted that the reaction did not proceed at room temperature. Interestingly, in the absence of a base, the reaction exhibited the same efficiency.

The formation of the new compound **2a** was easily followed in ^{31}P NMR spectroscopy as a broad quartet was observed at 12.22 ppm (J_{P-B} = 186.1 Hz), which clearly demonstrated the formation of a B–P bond. Additionally, the ^{11}B NMR spectrum showed 4 signals at 14.62 ppm (d, J = 140 Hz, 1B), −9.98 ppm (d, J = 190 Hz, 1B), −22.62 ppm (d, J = 131 Hz, 4B) and −25.79 ppm (d, J = 131 Hz, 4B), which have the characteristic pattern of an apical-substituted decaborate cluster (Scheme 1).

With these conditions in hand, the scope of the reaction was then evaluated (Scheme 2).

Using 0.5 equiv. of $Pd(PR_3)_2$ precursors (PR_3 = P(*o*-tolyl)$_3$, P(*m*-Cl-C_6H_4)$_3$ and P(cyclohexyl)$_3$), the corresponding [N(*n*-C_4H_9)$_4$][1-$B_{10}H_9PR_3$] derivatives were obtained in high isolated yields after 0.5–3 h of reaction at 50 °C (**2b**, 87%; **2d**, 76%; and **2e**, 75%). Noticeably, 0.5 equiv. of palladium precursors Pd$(PR_3)_2$ was used in order to find the equimolar ratio between the phosphines and the [*closo*-$B_{10}H_9$-1-I]$^{2-}$ derivative. To prepare compound **2c**, 35 mol% of Pd(3,5-$(CF_3)_2C_6H_3)_3P)_3$ was used. After 4 h at 50 °C, the corresponding [N(*n*-C_4H_9)$_4$][$B_{10}H_9$(3,5-$(CF_3)_2C_6H_3)_3$P)] derivative **4c** was isolated in 90% yield.

The availability of commercially available $Pd(PR_3)_n$ is low, and a search for an alternative method starting from phosphine and palladium precursors was carried out. Thus, using 12.5 mol% of $Pd_2(dba)_3$ and 1 equiv. of PPh_3 in THF at 50 °C for 2 h led to the same results as starting with $Pd(PPh_3)_4$ as the corresponding [N(*n*-C_4H_9)$_4$][1-$B_{10}H_9(PPh_3)$] **2a** was obtained in 80% isolated yield. Accordingly, the [N(*n*-C_4H_9)$_4$][1-$B_{10}H_9(PBn_3)$] compound **2f** was prepared starting from 25 mol% of Pd_2dba_3 and 1.0 equiv. of tribenzylphosphine and isolated in 83% yield.

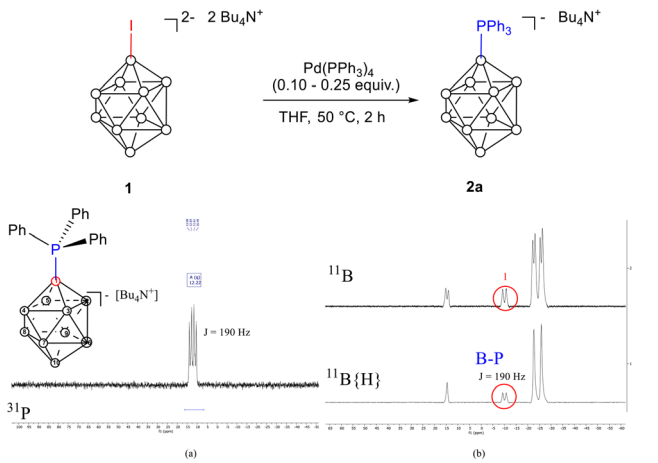

Scheme 1 Preparation of [N(*n*-C_4H_9)$_4$][1-$B_{10}H_9(PPh_3)$] **2a**. (a) ^{31}P NMR spectrum for [$B_{10}H_9PR_3$][N(*n*-C_4H_9)$_4$] **2a** and (b) ^{11}B NMR and ^{11}B{^{1}H} spectra for [$B_{10}H_9PPh_3$][N(*n*-C_4H_9)$_4$] **2a**.

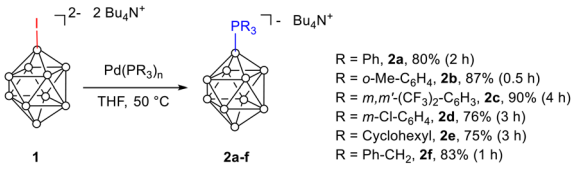

Scheme 2 Scope of the reaction.

Characterization of compounds 2a–f

Mass spectrometry studies. The new compounds **2a–f** were characterized by ESI-MS mass spectrometry. Molecular ions were consistent with the presence of the expected [N(*n*-C_4H_9)$_4$][1-$B_{10}H_9(PPh_3)$] complexes **2a–f** (see the ESI†).

NMR studies. **2a–f** exhibited NMR spectra consistent with the structures of the expected compounds (Scheme 1 and Table 1). Noticeably, in ^{31}P NMR spectra, a typical quartet with a coupling constant $^1J_{P-B}$ ranging from 180 to 190 Hz was observed for all the derivatives.[22,23] The boron cluster was also classically identified by ^{11}B NMR. The spectra exhibited a classical pattern for apical-substituted *closo*-decaborate with four peaks: (i) two doublets for the boron atoms in equatorial positions (a shift in the range from −20.0 to −27.0 ppm) and one doublet for the boron at the unsubstituted apical position (a shift in the range from 11.9 to 20.3 ppm), with $^1J_{B-H}$ coupling values in the range of 128–136 Hz; and (ii) one doublet for the substituted boron at the apical position (shift in the range from −8.4 to −14.1 ppm) with a coupling constant $^1J_{P-B}$ ranging from 180 to 190 Hz.[22,23]

IR studies. **2a–f** exhibited a characteristic broad intense peak at 2470–2490 cm^{-1} (ν, cm^{-1}: **2a**, 2491; **2b**, 2473; **2c**, 2485; **2d**, 2486; **2e**, 2470; **2f**, 2464).

X-ray crystal diffraction and molecular structures

Colorless monoclinic crystals of **2a**, **2b**, and **2f** and triclinic crystals of **2c**, **2d**, and **2e** were obtained from dichloromethane/diethyl ether solutions upon slow diffusion at 0 °C. Compounds **2a–f** were then characterized by X-ray diffraction. Molecular crystal structures are shown in Fig. 1. Most salts in the series have a single ion pair in the asymmetric unit, except for **2d** (two anions and two cations) and **2c** (four anions and four cations). The large [Bu_4N]$^+$ cation is disordered in most salts. For **2e**, the crystal is disordered with some constraints and **2c** shows disorder in the CF_3 group. The obtained crystal structure of **2d** is slightly twinned. The crystallographic data (bond lengths, angles, and torsion angles) are summarized in Tables 2, 3, and Table S1.†

The B–P bond lengths in **2a–2f** are in the range of 1.858–1.898 Å. These values are consistent with the ones described for similar substituted phosphine borane clusters such as 1.9055 and 1.91113 Å for 1,7-$(PMe_2Ph)_2$-*closo*-$B_{12}H_{10}$,[17] 1.901 and 1.886 Å for 2,8-$(PMe_2Ph)_2$-*closo*-$B_{10}H_8$ [23] or 1.928 Å for [$B_{12}H_{11}PPh_3$][N(*n*-C_4H_9)$_4$].[17] Nevertheless, the B–P bond lengths in **2a–2f** are slightly shorter than typical B–P single bonds (1.90–2.00 Å). Noticeably, in classical organophosphorus-borane derivatives, the B–P single-bond distance

Table 1 ^{31}P and ^{11}B NMR data for **2a–f**

	2a	2b	2c	2d	2e	2f
^{31}P NMR						
δ (ppm)	12.22	18.03	16.84	13.48	12.52	3.37
$^{1}J_{P-B}$ (Hz)	190	191	189	192	183	184
^{11}B NMR						
δ (ppm)	14.62	14.14	20.34	16.51	11.98	13.43
$^{1}J_{B-H}$ (Hz)	140	146	148	147	145	147
Integration	1B	1B	1B	1B	1B	1B
δ (ppm)	−9.98	−9.23	−14.08	−11.52	−12.12	−8.40
$^{1}J_{P-B}$ (Hz)	190	191	189	192	185	188
Integration	1B	1B	1B	1B	1B	1B
δ (ppm)	−22.62	−22.00	−20.89	−22.06	−24.48	−23.31
$^{1}J_{B-H}$ (Hz)	131	133	136	136	128	133
Integration	4B	4B	4B	4B	4B	4B
δ (ppm)	−25.79	−25.95	−24.85	−25.47	−26.68	−26.14
$^{1}J_{B-H}$ (Hz)	131	129	134	134	135	133
Integration	4B	4B	4B	4B	4B	4B

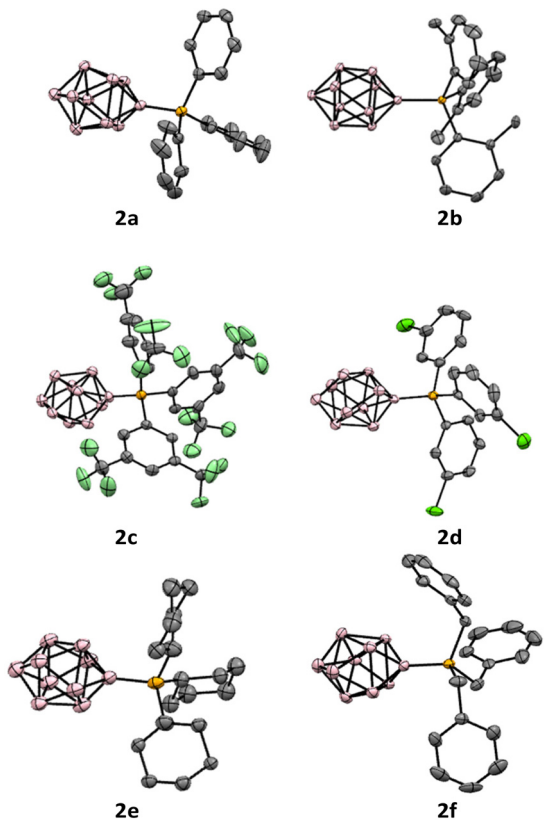

Fig. 1 Crystal structures (50% probability level for the displacement ellipsoids) of **2a–f**. Tetrabutylammonium counterions and hydrogen atoms are omitted for clarity. In **2d** and **2c**, only one unique molecule is shown.

range is 1.90–2.00 Å and the double-bond distance range is 1.79–1.84 Å.[25] Such observations can be explained by potential π-overlap between the boron and phosphorus atoms.[26]

P–$C_{\alpha\text{-carbons}}$ bond lengths in **2a–f** (from 1.805 to 1.835 Å) aligned with expected values for phosphorus–carbon single bonds. The expected bond length for P–C in a phosphine is approximately 1.80–1.85 Å, with slight variations depending on the specific electronic and steric environments.[17,22,23]

Within the boron cluster, the B–B bond lengths in **2a–f** ranged from 1.66 to 1.70 Å, which is consistent with the expected range for boron hydride clusters (typically in the range of 1.6–1.8 Å), reflecting normal bonding interactions.[27] Measurements of distances between apical boron atoms and the equatorial plane revealed that the substitution at the B_1 position with the phosphorus group induced slight contraction of the boron cage (average 1.067 Å compared to 1.093 Å for the unsubstituted $B_{10}H_{10}^{2-}$ motif). This contraction likely arises from electron-withdrawing effects or steric interactions associated with the phosphorus substituent. In contrast, B_{10}, which remains unsubstituted, retained a geometry similar to that of the unsubstituted cluster, showing no significant distortion.

The bond angles around the phosphorus centre deviated from the ideal tetrahedral geometry. As a representative example, in the crystal structure of **2d**, the angles between the phenyl groups (C_1–P_1–C_{13} = 106.4(2)°, C_1–P_1–C_7 = 106.5(2)°, and C_{13}–P_1–C_7 = 105.6(2)°) were compressed relative to the ideal 109.5°. In contrast, the bond angles of the cluster (C_1–P_1–B_1 = 111.6(2)°, C_7–P_1–B_1 = 114.2(2)°, and C_{13}–P_1–B_1 = 112.0(3)°) are larger than the ideal tetrahedral angle. This widening can be attributed to the steric bulk of the $B_{10}H_9$ cluster, which exerts significant repulsive force, pushing the phenyl groups away from the cluster, resulting in increased bond angles. This trend is similar for the rest of the **2a–2f** series.

Mechanism studies

First of all, in order to confirm or exclude the involvement of radicals during the transformation, several radical scavengers

Table 2 Selected bond lengths (Å) for the series **2a–f**

Selected bond lengths (Å)						
	2a	**2b**	**2c**	**2d**	**2e**	**2f**
P–B	P_1–B_1 = 1.870(3)	P_1–B_1 = 1.898(3)	P_1–B_1 = 1.864(6)	P_1–B_1 = 1.858(6)	P_1–B_1 = 1.876(5)	P_1–B_1 = 1.871(5)
P–C	P_1–C_1 = 1.807(2) P_1–C_{13} = 1.809(2) P_1–C_7 = 1.811(2)	P_1–C_8 = 1.821(3) P_1–C_{15} = 1.829(3) P_1–C_1 = 1.829(3)	P_1–C_9 = 1.812(5) P_1–C_1 = 1.816(5) P_1–C_{17} = 1.819(5)	P_1–C_{13} = 1.805(5) P_1–C_7 = 1.806(5) P_1–C_1 = 1.835(5)	P_1–$C_{13B/A}$ = 1.826(5) P_1–$C_{7B/A}$ = 1.833(5) P_1–$C_{1A/B}$ = 1.833(5)	P_1–C_{15} = 1.823(4) P_1–C_1 = 1.823(5) P_1–C_8 = 1.827(5)
B–B	B_1–B_4 = 1.686(4) B_1–B_5 = 1.686(4) B_1–B_3 = 1.692(4) B_1–B_2 = 1.692(4)	B_1–B_4 = 1.688(4) B_1–B_5 = 1.695(5) B_1–B_3 = 1.698(4) B_1–B_2 = 1.700(5)	B_1–B_4 = 1.686(8) B_1–B_5 = 1.685(8) B_1–B_3 = 1.677(8) B_1–B_2 = 1.693(8)	B_1–B_4 = 1.686(8) B_1–B_5 = 1.666(8) B_1–B_3 = 1.701(8) B_1–B_2 = 1.686(8)	B_1–B_4 = 1.692(7) B_1–B_5 = 1.698(7) B_1–B_3 = 1.684(7) B_1–B_2 = 1.693(8)	B_1–B_4 = 1.676(7) B_1–B_5 = 1.681(7) B_1–B_3 = 1.675(7) B_1–B_2 = 1.680(7)

Table 3 Selected angles (°) of the series **2a–f**

Selected angles (°)					
2a	**2b**	**2c**	**2d**	**2e**	**2f**
C_1–P_1–C_{13} = 107.95(12)	C_8–P_1–C_{15} = 105.27(13)	C_9–P_1–C_1 = 105.8(2)	C_{13}–P_1–C_7 = 105.6(2)	$C_{13B/A}$–P_1–$C_{7B/A}$ = 104.7(2)	C_{15}–P_1–C_1 = 103.5(2)
C_1–P_1–C_7 = 104.40(11)	C_8–P_1–C_1 = 106.24(13)	C_9–P_1–C_{17} = 105.8(2)	C_{13}–P_1–C_1 = 106.4(2)	$C_{13A/B}$–P_1–$C_{1A/B}$ = 110.9(2)	C_{15}–P_1–C_8 = 103.9(2)
C_{13}–P_1–C_7 = 107.03(11)	C_{15}–P_1–C_1 = 107.78(14)	C_1–P_1–C_{17} = 103.5(2)	C_7–P_1–C_1 = 106.5(2)	$C_{7A/B}$–P_1–$C_{1A/B}$ = 106.3(2)	C_1–P_1–C_8 = 106.1(2)
C_1–P_1–B_1 = 115.12(12)	C_8–P_1–B_1 = 112.77(14)	C_9–P_1–B_1 = 114.5(2)	C_{13}–P_1–B_1 = 112.0(3)	$C_{13B/A}$–P_1–B_1 = 111.2(2)	C_{15}–P_1–B_1 = 113.7(2)
C_{13}–P_1–B_1 = 109.26(12)	C_1–P_1–B_1 = 114.09(14)	C_1–P_1–B_1 = 114.1(2)	C_7–P_1–B_1 = 114.2(2)	$C_{7B/A}$–P_1–B_1 = 112.1(2)	C_1–P_1–B_1 = 115.7(2)
C_7–P_1–B_1 = 112.65(12)	C_{15}–P_1–B_1 = 110.23(14)	C_{17}–P_1–B_1 = 112.2(2)	C_1–P_1–B_1 = 111.6(2)	$C_{1A/B}$–P_1–B_1 = 111.5(2)	C_8–P_1–B_1 = 112.7(2)

such as 2,2,6,6-tetramethylpiperidinyloxyl (TEMPO), 2,6-di-*tert*-butyl-4-methyl-phenol (BHT) and galvinoxyl free radicals, have been used as additives. Thus, conducting the reaction of $[NBu_4]_2[B_{10}H_9I]$ **1** (1 equiv.) with $Pd(PPh_3)_4$ (25 mol%) in the presence of a radical scavenger (1 equiv.) in THF at 50 °C for 2 h led to the corresponding compound **2a** without loss of activity, which excluded a radical pathway.

To monitor the reaction progress, both ^1H and ^{31}P NMR spectra were recorded. First of all, the formation of the $[N(n\text{-}C_4H_9)_4][1\text{-}B_{10}H_9(PPh_3)]$ product **2a** was monitored by ^1H-NMR depending on the temperature. At temperatures lower than 55 °C, no reaction occurred as confirmed by the presence of the characteristic signals δ = 7.25, δ = 7.19, and δ = 7.09 ppm of $Pd(PPh_3)_4$. After 15 min at 55 °C, $Pd(PPh_3)_4$ was fully transformed and product **2a** was selectively obtained (aromatic signals at 7.98–7.88 and 7.60–7.45) (Fig. 2).

Interestingly, when conducting the reaction with $Pd(PPh_3)_4$ and *closo*-$[Bu_4N]_2[1\text{-}B_{10}H_9I]$ **1** in the presence of excess triphenylphosphine, no reaction occurred. This may suggest that the excess phosphine disfavoured the dissociation of the PPh_3 ligand from $Pd(PPh_3)_4$ in order to generate an active species able to promote an oxidative addition step. Additionally, during the substrate scope investigation, the electronic nature of substituents on the phosphine significantly affected the kinetics of the reaction. When an electron-donating substituent was used (*e.g.*, $-CH_3$ of the tolyl group in **4b**), the reaction time was reduced to 30 minutes. In contrast, using a phosphine with an electron-withdrawing group, such as CF_3 (complex **4c**) or chlorine (complex **4d**), led to a slower transformation with a reaction time extended to 4 and 3 hours, respectively. Indeed, phosphines bearing electron-withdrawing substituents should disfavour the oxidative addition, which thus seems an important step. With tricyclohexylphosphine palladium species, the reaction time was 3 h, showing that the hindrance of phosphine slowed down the reaction. Such observations may indicate that the oxidative step was involved and was the kinetic key step. It should be also noted that *n*-Bu_4NI crystals were isolated from the crude mixture obtained at the end of the reaction conducted under optimized conditions.

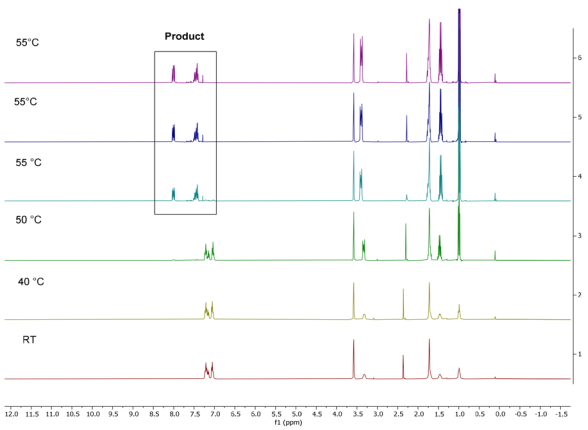

Fig. 2 ^1H NMR spectra for the reaction mixture between $[N(n\text{-}C_4H_9)_4]_2[B_{10}H_9I]$ and $Pd(PPh_3)_4$ in d^8-THF after 15 min at RT, 313 K (40 °C), 323 K (50 °C) and 328 K (55 °C).

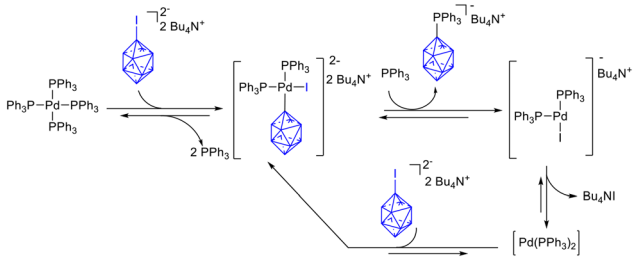

Scheme 3 Proposed mechanism for the reaction of the phosphine complex with $[N(n\text{-}C_4H_9)_4]$ $[B_{10}H_9I]$.

A plausible mechanism can be proposed when starting from the 18-electron complex $Pd(PPh_3)_4$; after non-reductive elimination of two phosphine ligands followed by the oxidative addition of the $[B_{10}H_9I]^-$ anion, a palladium(0) $[Bu_4N]_2[(1\text{-}B_{10}H_9)(I)Pd(PPh_3)_2]$ species was obtained. Due to steric hindrance caused by the presence of the decaborate entity and phosphine ligands, this latter complex should lead to an unusual elimination of $[Bu_4N][(1\text{-}B_{10}H_9)(PPh_3)]$ and after coordination of PPh_3 gave the anionic species $[Pd(I)(PPh_3)_2]^-$, which after elimination of n-Bu_4NI generated $Pd(PPh_3)_2$ that was able to perform a second oxidative addition of the *closo*-$[Bu_4N]_2[1\text{-}B_{10}H_9I]$ cluster.[28] Nevertheless, it cannot be excluded that the tricoordinated anionic species $[Pd(I)(PPh_3)_2]^-$ performed an oxidative addition with *closo*-$[Bu_4N]_2[1\text{-}B_{10}H_9I]$, thus leading to a pentacoordinated intermediate despite steric hindrance of the cluster (Scheme 3).[29–32]

Conclusions

We have developed a simple, convenient and efficient method for the preparation of mono-anionic phosphine derivatives of a *closo*-decaborate cluster starting from the *closo*-$[Bu_4N]_2[1\text{-}B_{10}H_9I]$ cluster using an equimolar amount of the desired phosphine ligand associated with the Pd^0 precursor. Both triaryl- and tri-alkyl phosphine clusters can be prepared with high selectivity and yields. Noticeably, the obtained phosphine clusters were characterized by NMR, HR-MS, IR and X-ray diffraction studies. Based on the experiments, a mechanistic pathway was proposed, suggesting notably the role of palladium(0) involved in the key step oxidative addition of the B–I bond.

Conflicts of interest

There are no conflicts to declare.

Data availability

Crystallographic data for compounds **2a–2f** have been deposited at the CCDC under deposition numbers 2456501–2456506† and can be obtained from **https://www.ccdc.cam.ac.uk**. All other data including NMR spectra supporting this article have been included as part of the ESI.†

Acknowledgements

We wish to acknowledge the Université de Rennes (France), the Centre National de la Recherche Scientifique (CNRS, France), the Lebanese University (Lebanon), and CNRSL (Lebanon).

References

1 (*a*) N. S. Hosmane, *Boron Science. New Technologies and Applications*, Taylor & Francis Books/CRC Press, Boca Raton, 2016; (*b*) R. N. Grimes, *Carboranes*, Elsevier Science, Amsterdam, 2016; (*c*) N. S. Hosmane and R. D. Eagling, *Handbook of Boron Science: With Applications in Organometallics, Catalysis, Materials and Medicine (In 4 Volumes)*, World Scientific, London, UK, 2018; (*d*) L. Mcconnell, *Boron: Advances in Research and Applications*, Nova Science Publishers, 2021; (*e*) Y. Zhu, *Fundamentals and Applications of Boron Chemistry*, Elsevier, 2022; (*f*) M. F. Hawthorne, *Boranes and beyond: History and the man who created them*, Springer Nature, 2023.
2 I. B. Sivaev, A. V. Prikaznov and D. Naoufal, *Collect. Czech. Chem. Commun.*, 2010, **75**, 1149–1199.
3 W. C. Ewing, *6- and 5-Halodecaboranes: Selective Syntheses from ClOSO-B10H10 (2-) and Use as Polyborane Building Blocks*, 2010.
4 Z. Laila, F. Abi-Ghaida, S. Al Anwar, O. Yazbeck, R. Jahjah, R. Aoun, S. Tlais, A. Mehdi and D. Naoufal, *Main Group Chem.*, 2015, **14**, 301–312.
5 N. Mahfouz, F. Abi-Ghaida, F. A. Ghaida, Z. El Hajj, M. Diab, S. Floquet, A. Mehdi and D. Naoufal, *ChemistrySelect*, 2022, **7**, e202200770.
6 V. V. Voinova, I. N. Klyukin, A. S. Novikov, A. Y. Kozmenkova, A. P. Zhdanov, K. Y. Zhizhin and N. T. Kuznetsov, *Russ. J. Inorg. Chem.*, 2021, **66**, 295–304.
7 V. M. Retivov, E. Y. Matveev, M. V. Lisovskiy, G. A. Razgonyaeva, L. I. Ochertyanova, K. Y. Zhizhin and N. T. Kuznetsova, *Russ. Chem. Bull.*, 2010, **59**, 550–555.
8 Z. Laila, O. Yazbeck, F. Abi Ghaida, M. Diab, S. El Anwar, M. Srour, A. Mehdi and D. Naoufal, *J. Organomet. Chem.*, 2020, **910**, 121132.
9 D. Naoufal, Z. Assi, E. Abdelhai, G. Ibrahim, O. Yazbeck, A. Hachem, H. Abdallah and M. El Masri, *Inorg. Chim. Acta*, 2012, **383**, 33–37.
10 H. Hatanaka, *J. Neurol.*, 1975, **209**, 81–94.
11 C. Salt, A. J. Lennox, M. Takagaki, J. A. Maguire and N. S. Hosmane, *Russ. Chem. Bull.*, 2004, 1871–1888.
12 Z. Yinghuai, Boron-Based Hybrid Nanostructures: Novel Applications of Modern Materials, in *Hybrid Nanomaterials: Synthesis, Characterization, and Applications*, eds. B. P. S.

Chauhan, John Wiley & Sons, Inc., 1st edn, 2011, pp. 181–198.
13 D. Naoufal, B. Grüner, P. Selucký, B. Bonnetot and H. Mongeot, *J. Radioanal. Nucl. Chem.*, 2005, **266**, 145–148.
14 K. E. Yorov, A. P. Zhdanov, R. K. Kamilov, A. E. Baranchikov, G. P. Kopitsa, O. I. Pokrovskiy, A. L. Popov, O. S. Ivanova, L. Almásy, Y. G. Kolyagin, K. Y. Zhizhin and V. K. Ivanov, *ACS Appl. Nano Mater.*, 2022, **5**, 11529–11538.
15 A. Gigante, L. Duchêne, R. Moury, M. Pupier, A. Remhof and H. Hagemann, *ChemSusChem*, 2019, **12**, 4832–4837.
16 L. Jacob, E. Rzeszotarska, M. Koyioni, R. Jakubowski, D. Pociecha, A. Pietrzak and P. Kaszyński, *Chem. Mater.*, 2022, **34**, 6476–6491.
17 R. Bernard, D. Cornu, D. Luneau, D. Naoufal, J.-P. Scharff and P. Miele, *J. Organomet. Chem.*, 2005, **690**, 2745–2749.
18 H. C. Miller, N. E. Miller and E. L. Muetterties, *Inorg. Chem.*, 1964, **3**, 1456–1463.
19 S. A. Jasper, J. Mattern, J. C. Huffman and L. J. Todd, *Polyhedron*, 2007, **26**, 3793–3798.
20 J. F. Kleinsasser, E. D. Reinhart, J. Estrada, R. F. Jordan and V. Lavallo, *Organometallics*, 2018, **37**, 4773–4783.
21 A. M. Spokoyny, C. D. Lewis, G. Teverovskiy and S. L. Buchwald, *Organometallics*, 2012, **31**, 8478–8481.
22 D. Naoufal, B. Bonnetot, H. Mongeot and B. Grüner, *Collect. Czech. Chem. Commun.*, 1999, **64**, 856–864.
23 S. A. Jasper, R. B. Jones, J. Mattern, J. C. Huffman and L. J. Todd, *Inorg. Chem.*, 1994, **33**, 5620–5624.
24 E. Rzeszotarska, I. Novozhilova and P. Kaszyński, *Inorg. Chem.*, 2017, **56**, 14351–14356.
25 R. T. Paine and H. Noth, *Chem. Rev.*, 1995, **95**, 343–379.
26 D. C. Pestana and P. P. Power, *J. Am. Chem. Soc.*, 1991, **113**, 8426–8437.
27 Y.-F. Shen, C. Xu and L.-J. Cheng, *RSC Adv.*, 2017, **7**, 36755–36764.
28 S. Bouquillon, A. du Moulinet d'Hardemare, M.-T. Averbuch-Pouchot, F. Hénin and J. Muzart, *Polyhedron*, 1999, **18**, 3511–3516.
29 C. Amatore, M. Azzabi and A. Jutand, *J. Am. Chem. Soc.*, 1991, **113**, 8375–8384.
30 C. Amatore, E. Carré, A. Jutand, H. Tanaka, Q. Ren and S. Tori, *Chem. – Eur. J.*, 1996, **2**, 957–966.
31 C. Amatore and A. Jutand, *J. Organomet. Chem.*, 1999, **576**, 254–278.
32 C. Amatore and A. Jutand, *Acc. Chem. Res.*, 2000, **33**, 314–321.